An Efficient Beamformer for Interference Suppression Using Rectangular Antenna Arrays

H. M. Kha, T. V. Luyen*, and N. V. Cuong

Hanoi University of Industry, Hanoi, Vietnam; Email: khahoang@haui.edu.vn; luyentv@haui.edu.vn; cuongnv@haui.edu.vn

*Correspondence: luyentv@haui.edu.vn

***Abstract* —Over the past ten years, the development of fifth-generation cellular network technology opens the door to the deployment of huge sensors inside the Internet of Things (IoT), challenging the technologies of communications. IoT establishes wireless communication between numerous physical things to connect them over the Internet, as a result, these things may seriously pollute the environment for electromagnetic propagation. This paper proposes an efficient beamformer based on binary bat algorithm for interference suppression in wireless technology applications. The proposed beamformer utilizes the technique of controlling only the phase of excitation weights in uniform rectangular arrays. This beamformer can produce optimal patterns with minimal distortions in sidelobe regions while maintaining the main lobe and placing nulls in the direction of interfering signals. To demonstrate this ability, the proposed beamformer is evaluated through several scenarios and compared to a beamformer based on Binary Particle Swarm Optimization (BPSO). The results show that the proposed beamformer maintains the main lobe toward the desired user direction while imposing nulls in unwanted user directions (interferences) and that it surpassed BPSO-based beamformers in terms of convergence speed and interference suppression ability.**

***Keywords*—Beamforming, interference suppression, pattern nulling, uniform rectangular arrays, binary bat algorithm**

I. INTRODUCTION

Due to the increasing pollution of the electromagnetic environment, various kinds of interferences are serious concerns in communication system design and operation. To improve the ability of interference suppression and spectrum utilization in radar and wireless communications applications, array pattern synthesis and pattern nulling have been taken into account in numerous research papers. Several pattern nulling techniques including weight control, position-only control, and array thinning have been adopted to mitigate interferences with their merits and demerits. In smart antenna systems, adaptive beamformers based on weight control for interference suppression are of great interest and becoming important [1, 2]. In excitation weight-based controls, the phase-only control is the simplest, and it is easy to steer the main lobe; in addition, this control can be applied to existing phased array systems without incurring additional costs [2–4].

Recently, metaheuristic algorithms for optimization such as bat algorithm, particle swarm optimization, and genetic algorithm to solve continuous optimization problems or Binary Particle Swarm Optimization (BPSO) and Binary Bat Algorithm (BBA) to solve discrete optimization problems have all been proved to be effective global optimization algorithms to obtain optimal patterns [3–6]. Specifically, adaptive beamformers utilizing bat algorithm (or BBA) were successfully performed for uniform linear arrays, and the results shown that BBA-based and bat algorithm-based beamformers were proved to be superior to genetic algorithm-based and accelerated particle swarm optimization-based (or BPSO-based) ones in respect of pattern nulling [7, 8]. By using BBA or BPSO, binary numbers optimized by these algorithms can be directly applied to digital attenuators or digital phase shifters to control amplitudes and/or phases excited at each element.

The aforementioned beamformers were used for uniform linear arrays, but this type of array lacks the capability of scanning in 3D space [9]. In contrast, the main lobe of the pattern of uniform rectangular arrays (URAs) can be steered toward any direction of elevation and azimuth in space. In addition, URAs are more adaptable and can produce more symmetrical patterns with deeper sidelobes. Moreover, these arrays are more attractive for mobile devices and applications including tracking radar, search radar, remote sensing, and communications, especially for Internet of Things (IoT) applications using wireless communications [9–11].

With expanded coverage, higher throughput, reduced latency, and connection density of massive bandwidth, the evolution of Fifth-Generation (5G) networks is becoming a significant driving factor for the development of IoT and opening the door for the connection of billions of sensors via the Internet [12–14]. Additionally, Multiple-Input and Multiple-Output (MIMO) antennas in the form of smart antennas or beamforming are used in 5G wireless technology because they have the potential to suppress interferences and improve spectral efficiency in IoT applications for both transmitters and receivers [10], [15–17]. Moreover, the delay spread can be significantly decreased by using MIMO antennas. Thus, a promising technology that delivers significant bandwidth with

Manuscript received July 12, 2022; revised November 22, 2022; accepted January 23, 2023.

reduced transmission power requirements is beamforming with interference suppression capability. The main criteria for 5G IoT are secure communication, improved efficiency, and transmission of massive amounts of data without any interference [10, 18]. Because of this, interference suppression solution with fast response time is essential to 5G wireless communication technology [19].

In wireless technology applications, to handle the high traffic rate, scarcity of bandwidth, high-frequency bands, and wide signal bandwidth are required to increase the transmission bit rates, thereby providing better coverage with low power consumption at low cost. To achieve these objectives, microstrip patch antennas are essential to support mobile terminals of wireless communication systems because they are (i) easy to design, fabricate and integrate with other electronic devices, (ii) a cost-effective choice owing to the capability of fabricating on a variety of cheap substrates, and (iii) rugged and low profile. These characteristics are ideal for some practical applications such as GPS receivers, tablets, personal digital assistants, and so on [20]. Understanding these characteristics, this paper proposes a beamformer (BF) that utilizes the phase-only control and the basic BBA to suppress interferences. The proposed beamformer is verified by using URAs of patch antennas and by comparing it to a BPSO-based beamformer in terms of maintaining the main lobe, suppressing sidelobe levels (SLLs), and imposing nulls.

II. Problem Formulation

This paper considers a URA with $M \times N$ elements (blue dots) located as shown in Fig. 1. The antenna array pattern can be expressed as [9]:

$$P(\phi,\theta) = EF \cdot AF = EF \sum_{m=0}^{M-1} \sum_{n=0}^{N-1} w_{m,n} e^{j\left(m\psi_z + n\psi_y\right)}, \qquad (1)$$

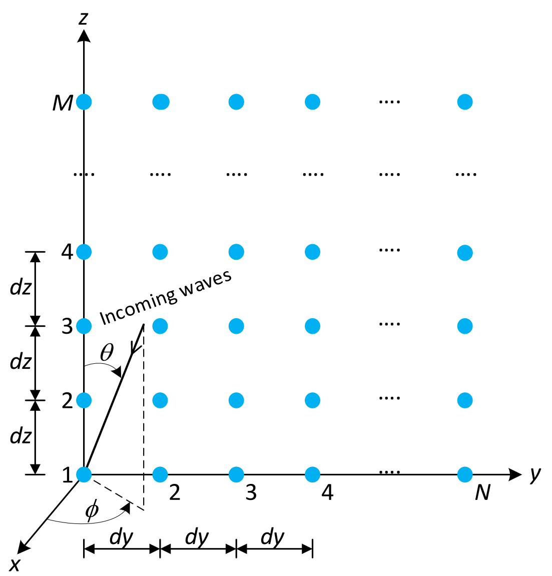

Figure 1. A URA with $M \times N$ elements.

where:

- EF and AF are the element factor of the element and the array factor of the array at (ϕ,θ), respectively;
- $\psi_z = \kappa d_z \cos(\theta)$; $\psi_y = \kappa d_y \sin(\theta)\sin(\phi)$;
- $\kappa = 2\pi / \lambda$ is the wave number;
- $w_{m,n} = a_{m,n} e^{j\delta_{m,n}}$ is the complex weight excited at the (m,n)th element; $a_{m,n}$ and $\delta_{m,n}$ are the amplitude and the phase, respectively.

To steer the main lobe toward (ϕ_0,θ_0), the phase shift of the (m,n)th element is equal to [9]:

$$\delta_{m,n} = -\kappa\left(md_z \cos(\theta_0) + nd_y \sin(\theta_0)\sin(\phi_0)\right). \qquad (2)$$

To obtain nulled patterns, optimal phases excited at each element can be acquired by using the proposed algorithm in the next section.

III. Efficient Beamformers for Interference Suppression

A. The Fitness Function

The fitness function in this proposal is developed for the receiver, but this development is similar for the transmitter. This function is built according to the following manners. Firstly, the proposed beamformer requires suppressing interferences while maintaining the main lobe and keeping sidelobes at a predefined level. This means that a problem required to solve is a constrained optimization problem. By applying the penalty method in [21], therefore, the constrained problem is converted into the unconstrained problem. The second one, if the main lobe is steered toward (ϕ_0,θ_0), most of the high-magnitude sidelobes occur at $(\phi = [-180° : 180°], \theta = \theta_0)$ and $(\phi = \phi_0, \theta = [0° : 180°])$. Nulls can be arbitrarily placed in 3D space, however, interferences emerging in high-magnitude sidelobes are the most undesirable, so this paper assumes that interferences emerge at $(\phi = [-90° : 90°], \theta = \theta_0)$. Therefore, the fitness function to solve the unconstrained problem can be formulated as follows:

$$F(\delta) = \frac{1}{\xi}\begin{bmatrix} \xi \sum_{i=1}^{I}\left[\left|P_o(\phi_i,\theta_i)\right|^2\right] + \\ \sum_{\phi=\phi_0,\theta=0°}^{\theta=180°}\left[\left|P_o(\phi,\theta) - P_r(\phi,\theta)\right|^2\right] + \\ \sum_{\theta=\theta_0,\phi=-90°}^{\phi=90°}\left[\left|P_o(\phi,\theta) - P_r(\phi,\theta)\right|^2\right] \end{bmatrix}, \qquad (3)$$

where:

- ξ is the penalty parameter that is chosen based on the first simulation scenario presented in the next section;
- I is the total number of interfering signals;
- (ϕ_i, θ_i) is the direction of the i^{th} interfering signal;
- $\xi \sum_{i=1}^{I} \left[\left| P_o(\phi_i, \theta_i) \right|^2 \right]$ is used to place I nulls at (ϕ_i, θ_i);
- $\sum_{\phi=\phi_0, \theta=0°}^{\theta=180°} \left[\left| P_o(\phi,\theta) - P_r(\phi,\theta) \right|^2 \right] + \sum_{\theta=\theta_0, \phi=-90°}^{\phi=90°} \left[\left| P_o(\phi,\theta) - P_r(\phi,\theta) \right|^2 \right]$ for $(\phi,\theta) \neq (\phi_i,\theta_i)$ are used to maintain the optimized pattern $P_o(\phi,\theta)$ with as little disturbance as possible concerning the reference pattern $P_r(\phi,\theta)$;
- $P_o(\phi,\theta)$ and $P_o(\phi_i,\theta_i)$ are patterns optimized by BPSO or BBA at (ϕ,θ) and (ϕ_i,θ_i), respectively;
- δ is the phase shift of elements in the array, and a is fixed as reference weights which produce $P_r(\phi,\theta)$.
- $P_r(\phi,\theta)$, $P_o(\phi,\theta)$, and $P_o(\phi_i,\theta_i)$ are calculated by using Eq. (1).

B. *The Proposed Algorithm*

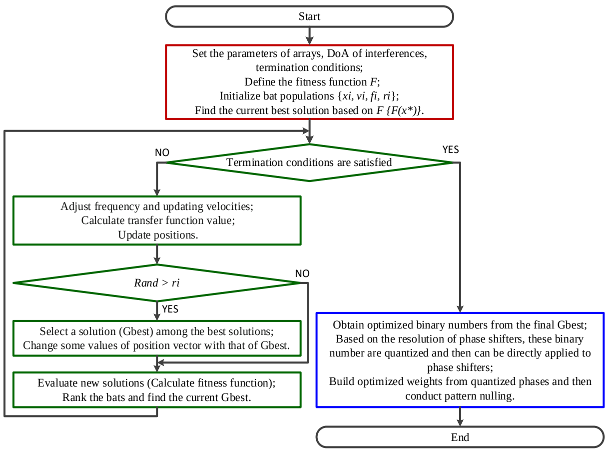

Figure 2. The flowchart of the proposed algorithm.

To obtain optimized weights, the proposed algorithm, which is displayed in Fig. 2, is implemented. This algorithm can be explained as follows: firstly, the parameters of BBA and the antenna array (a block with a red border) are initialized. After that, the search mechanism of BBA (blocks with a green border) is implemented (see more details in [22]). At the new solution evaluation or fitness function calculation, binary numbers are quantized based on the resolution of phase shifters, and then phase shifts (δ) in real numbers for elements in the array are obtained. Thereby, optimized weights are built, and the value of the fitness function is calculated by using Eq. (3). Finally, optimized weights are acquired to form nulled patterns (a block with a blue border).

IV. Results and Discussion

In this section, the performance of the proposal for interference suppression is evaluated via four scenarios. The CST Studio Suite 2019 is used to design patch antennas with a resonant frequency of 2.4 GHz for URAs and to simulate mutual coupling effects on optimized patterns. The characteristics of a designed patch antenna, which include dimensions, 3D pattern, and the S_{11} parameter, are shown in Fig. 3.

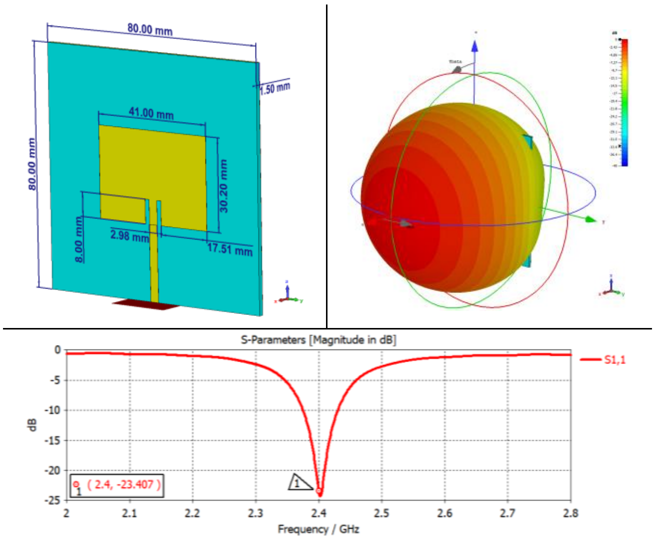

Figure 3. The characteristics of a patch antenna designed in CST.

Common parameters for all simulation scenarios:

- The element factor is the pattern of a patch antenna which is designed in Fig. 3.
- 6-bit digital phase shifters are used for the array of patch antennas with $M = N = 5$ and $d_y = d_z = 85$ millimeters.
- The reference pattern $P_r(\phi,\theta)$ is chosen as the Chebyshev pattern with $\text{SLL} = -25\,\text{dB}$.
- The population is 50, and the iteration is 2 from the third scenario onwards.
- The solutions of BBA and BPSO are randomly initialized apart from one solution initialized with 0.
- Because the initial solutions are random, the results for all scenarios will be calculated as the average values of 2000 independent simulations to verify the performance of two BFs based on BBA and BPSO.

- For simplicity, the parameters of BBA and BPSO are set as the recommendation of [22, 23]:
  BBA: $r = 0.5$, $f_{\min} = 0$ and $f_{\max} = 2$.
  BPSO: $C_1 = C_2 = 2$; $w = [0.4, 0.9]$; $V_{\max} = 6$.
  The transfer function is V-shaped.

A. *Penalty Parameter* ξ

The first scenario determines the penalty parameter ξ which is an unknown parameter in the fitness function. According to this function, if the penalty parameter values are too large, it may lead to over penalty, whereas too small values may lead to under penalty. To point out the right value of this parameter, the first null beamwidth (FNBW) and the null depth level (NDL) at $(\phi_i, \theta_i) = (45°, 90°)$ are evaluated with penalty parameter values from 10^0 to 10^5 with population $= 50$ and iteration $= 5$. The results, which are demonstrated in Fig. 4 and Fig. 5, indicate that the larger the value of ξ, the deeper the null, and the FNBW of optimized patterns also considerably changes when ξ is big enough. To balance the trade-off between NDL and FNBW, ξ should be 7500, and it is chosen for the next scenarios.

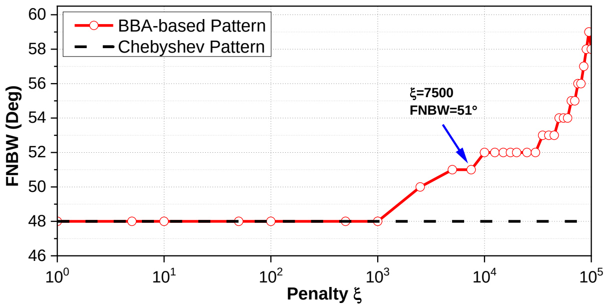

Figure 4. The FNBW of optimized pattern with different penalty values.

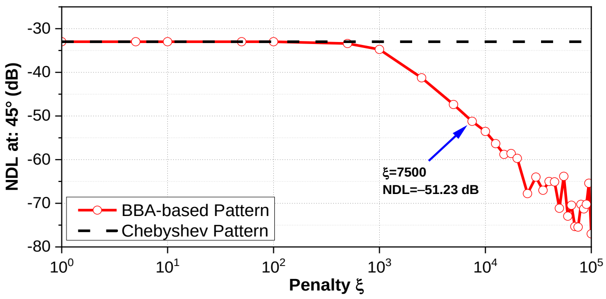

Figure 5. The NDL of optimized pattern with different penalty values.

B. *Convergence Characteristics*

This scenario compares the value of the fitness function in the case of placing a single null at a peak of the Chebyshev pattern $(\phi_i, \theta_i) = (45°, 90°)$. BBA-based BF is investigated with different population sizes over 200 iterations. Based on the results shown in Fig. 6, this beamformer has taken 16, 4, 2, and 2 iterations to approximately achieve $F \le 0.2$ corresponding to population $= 10$, 30, 50 and 70, respectively. For illustrative purposes, population $= 50$ and iteration $= 2$ are chosen for the next scenarios.

In addition, the fitness function of the proposed beamformer is compared to that of BPSO-based BF with population $= 50$ and iteration $= 150$, which is displayed in Fig. 7. Overall, the one based on BBA converges much more quickly than that based on BPSO. BBA-based BF requires about 50 iterations to nearly converge while BPSO-based BF still cannot converge after 150 iterations. At the 50th iteration, BBA-based BF achieved the value of 0.07854 whereas BBA-based BF only achieved the value of 0.2262. Furthermore, the value of the fitness function of BBA-based BF is lower than that of BPSO-based BF through the entire 150 iterations. Indeed, BBA-based BF only takes 85.09 milliseconds to achieve $F \le 0.2$ while BPSO-based BF requires 1026.12 milliseconds, which is 12 times longer than that of the proposed beamformer.

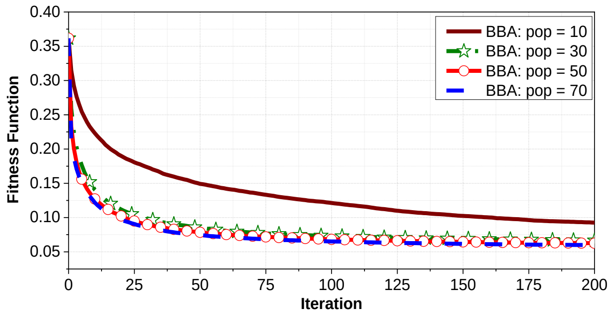

Figure 6. The fitness function of BBA-based BF with different population sizes.

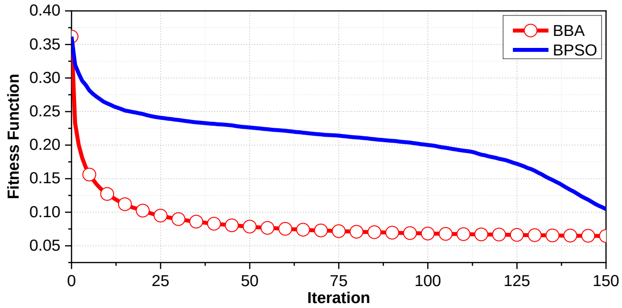

Figure 7. The fitness function of BFs based on BBA and BPSO.

C. *Efficient Null-Steering Ability*

This scenario presents the adaptive null-steering ability of the proposed beamformer when interfering signals emerge in a single direction, multiple directions, and a broad direction. Figs. 8-10 compare patterns optimized by BBA and BPSO with a single null, multiple nulls, and a broad null, respectively. In general, both BBA-based and BPSO-based BFs can maintain the main lobe relative to that of the Chebyshev pattern, with half-power beamwidth about 18° and FNBW about 51° compared to 16° and 48° of the Chebyshev pattern, respectively. However, BBA-based BF is superior to BPSO-based BF in terms of suppressing sidelobes as well as imposing nulls. Take the first case, for example, a single null at

$(\phi_i = 45°, \theta_i = 90°)$ imposed by the proposed beamformer is suppressed down to −50.26 dB whereas that by BPSO-based BF is only down to −36.61 dB. Similarly, the NDLs of multiple nulls at $(\phi_i = 30°; 50°, \theta_i = 90°)$ and a broad null at $(\phi_i = [40° : 50°], \theta_i = 90°)$ optimized by BBA-based BF are all deeper than that by BPSO-based one. Specifically, in Fig. 9, BBA-based BF imposed two nulls at $(\phi_i = 30°, \theta_i = 90°)$ and $(\phi_i = 50°, \theta_i = 90°)$ with $-47.58\,\text{dB}$ and $-45.17\,\text{dB}$ respectively while BPSO-based BF was with $-34.50\,\text{dB}$ and $-39.54\,\text{dB}$. In Fig. 10, the maximum radiated power between 40° and 50° in the pattern optimized by BBA-based BF and BPSO-based BF were $-47.74\,\text{dB}$ and $-40.67\,\text{dB}$, respectively. That is to say, the beamformer based on BBA has better interference suppression than that based on BPSO.

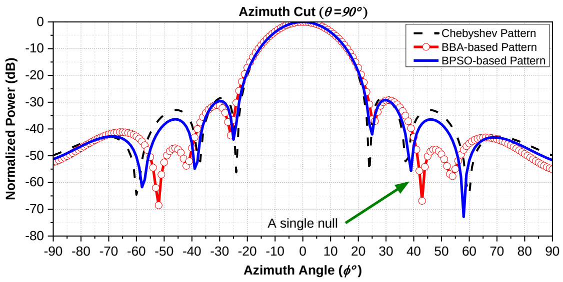

Figure 8. The 2D optimized patterns with a single null.

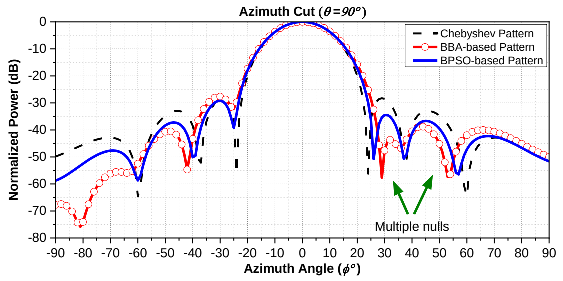

Figure 9. The 2D optimized patterns with multiple nulls.

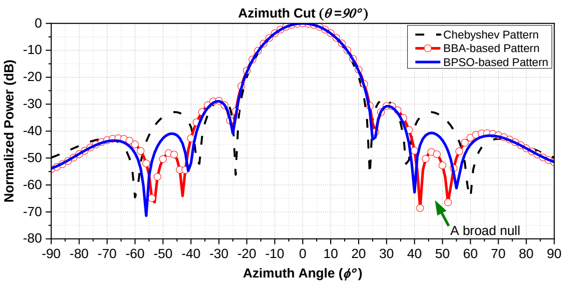

Figure 10. The 2D optimized patterns with a broad null.

D. *Optimized Patterns with the Different Resolutions of Phase Shifters*

The main lobe of the proposed beamformer not only is limited to the fixed direction as in the above scenarios but also can be steered by using Eq. (2). This is accomplished by steering the main lobe toward the desired direction before performing the aforementioned processes. In the last scenario, the proposed beamformer is verified in case of steering the main lobe toward $(\phi_0 = 10°, \theta_0 = 80°)$ while placing nulls in the range of $(\phi_i = [-40° : -30°], \theta_i = 80°)$. Besides, the efficiency of the proposal is also evaluated when using phase shifters with different resolutions and simulated in CST Studio Suite in which mutual coupling effects are taken into account. Firstly, the comparison of the 2D patterns in theory and simulation on CST is shown in Fig. 11. Although the main lobe, in theory, is equivalent to that in simulation on CST, it is difficult to suppress sidelobes. Also, sidelobes at $(\phi_i = [-40° : -30°], \theta_i = 80°)$ in the simulation on CST are still suppressed; however, those sidelobes are shallower than those in theory. Generally, although there are mutual coupling effects, BBA-based BF still can maintain the main lobe and suppress sidelobes in the region where interferences emerge.

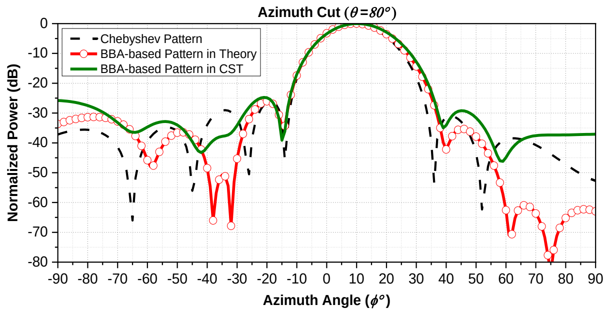

Figure 11. The 2D patterns when using 4-bit phase shifters.

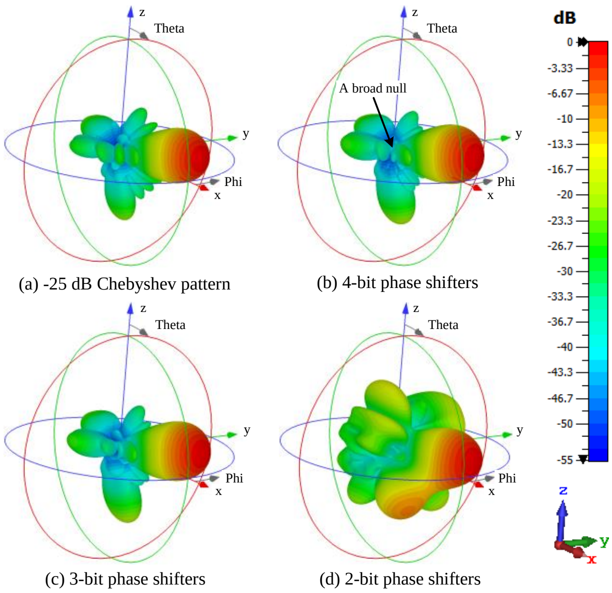

Figure 12. The 3D patterns with the different resolutions of phase shifters.

Secondly, the 3D Chebyshev pattern with $\text{SLL} = -25\,\text{dB}$ and 3D optimized patterns with different resolutions of phase shifters are demonstrated in Fig. 12. The results indicate that if the number of bits decreases, the SLLs increase, and more sidelobes appear. The resolution of phase shifters is proportional to the cost so to balance the trade-off between the cost and performance, phase shifters with 4 bits should be used.

V. Conclusion

This paper proposed a beamformer based on BBA for URAs of patch antennas. The ability to set nulls in sidelobe regions was verified via various simulation scenarios such as null-steering ability and the effect of the resolution of phase shifters and mutual coupling on optimized patterns. The paper suggested that BBA-based BF should use 4-bit phase shifters to balance the trade-off between cost and performance. Also, BBA-based BF was proven to outperform the BPSO-based one in terms of convergence speed and NDLs. In other words, BBA-based BF can suppress interferences better than BPSO-based one; for instance, BBA-based one converged 12 times faster than BPSO-based one to obtain optimized patterns, and the signal-to-interference ratio of BBA-based one was greater than that of BPSO-based one. It is expected that BBA-based BF can act as a promising and feasible solution for IoT applications and 5G wireless communication technology. For future works, unknown interferences, interferences entering the main lobe, mutual coupling compensation, convex optimization, or approaches for reducing the hardware requirements should be considered. Moreover, the solution in this paper should be studied for integrated sensing and communications technology in which the integration of radio sensing and communication systems allows for the effective use of limited resources and even the pursuit of mutually beneficial goals as well as the relevant enabling technologies.

Conflict of Interest

The authors declare no conflict of interest.

Author Contributions

All authors conducted the research; simulated and analyzed the data; wrote the paper, and all authors had approved the final version.

References

[1] G. Charis and N. Showme, “Beamforming in wireless communication standards: A survey,” *Indian Journal of Science and Technology*, vol. 10, no. 5, pp. 1–5, 2017.

[2] R. Haupt, *Antenna Arrays: A Computational Approach*, Hoboken, NJ, USA: Wiley, 2010, pp. 156–176, 484–515.

[3] T. V. Luyen and T. V. B. Giang, “Interference suppression of ULA antennas by phase-only control using bat algorithm,” *IEEE Antennas and Wireless Propagation Letters*, vol. 16, pp. 3038–3042, 2017.

[4] T. V. Luyen, H. M. Kha, N. V. Tuyen, and T. V. B. Giang, “An efficient ULA pattern nulling approach in the presence of unknown interference,” *Journal of Electromagnetic Waves and Applications*, vol. 35, no. 1, pp. 1–18, 2021.

[5] T. V. Luyen and T. V. B. Giang, “Null-steering beamformer using bat algorithm,” *Applied Computational Electromagnetics Society Journal*, vol. 33, no. 1, pp. 23–29, 2018.

[6] T. V. Luyen, N. V. Cuong, and L. Duy, “An effective beamformer for interference mitigation,” *Intelligent Systems and Networks, Springer Nature Singapore*, vol. 471, pp. 630–639, 2022.

[7] T. V. Luyen, *et al*., “Null-steering beamformers for suppressing unknown direction interferences in sidelobes,” *Journal of Communications*, vol. 17, no. 8, pp. 600–607, 2022.

[8] T. V. Luyen and N. V. Cuong, “An effective beamformer for interference suppression without knowing the direction,” *International Journal of Electrical and Computer Engineering*, vol. 13, no. 1, 2023.

[9] C. A. Balanis, *Antenna Theory: Analysis and Design, 4th ed.*, John Wiley and Sons, 2016, pp. 348–360.

[10] L. Chettri and R. Bera, “A comprehensive survey on Internet of Things (IoT) toward 5G wireless systems,” *IEEE Internet of Things Journal*, vol. 7, no. 1, pp. 16–32, 2020.

[11] M. K. Maheshwari, M. Agiwal, N. Saxena, and A. Roy, “Flexible beamforming in 5G wireless for Internet of Things,” *IETE Technical Review*, vol. 36, no. 1, pp. 3–16, 2017.

[12] D. Wang, D. Chen, B. Song, N. Guizani, X. Yu, and X. Du, “From IoT to 5G I-IoT: The next generation IoT-based intelligent algorithms and 5G technologies,” *IEEE Communications Magazine*, vol. 56, no. 10, pp. 114–120, 2018.

[13] V. K. Quy, N. V. Hau, D. V. Anh, and L. A. Ngoc, “Smart healthcare IoT applications based on fog computing: Architecture, applications and challenges,” *Complex & Intelligent Systems. Springer Science and Business Media LLC*, 2021.

[14] Q. V. Khanh, N. V. Hoai, L. D. Manh, A. N. Le, and G. Jeon, “Wireless communication technologies for IoT in 5G: Vision, applications, and challenges,” *Wireless Communications and Mobile Computing*, vol. 2022. Hindawi Limited, pp. 1–12, 2022.

[15] K. Shafique, B. A. Khawaja, F. Sabir, S. Qazi, and M. Mustaqim, “Internet of Things (IoT) for next-generation smart systems: A review of current challenges, future trends and prospects for emerging 5G-IoT scenarios,” *IEEE Access*, vol. 8, pp. 23022–23040, 2020.

[16] I. Ahmed, *et al*., “A survey on hybrid beamforming techniques in 5G: Architecture and system model perspectives,” *IEEE Communications Surveys & Tutorials*, vol. 20, no. 4, pp. 3060–3097, 2018.

[17] X. Zhu, F. Qi, and Y. Feng, “Deep-learning-based multiple beamforming for 5G UAV IoT networks,” *IEEE Network*, vol. 34, no. 5, pp. 32–38, 2020.

[18] K. S. Mohamed, M. Y. Alias, M. Roslee, and Y. M. Raji, “Towards green communication in 5G systems: Survey on beamforming concept,” *IET Communications*, vol. 15, no. 1, pp. 142–154, 2020.

[19] M. U. A. Siddiqui, F. Qamar, F. Ahmed, Q. N. Nguyen, and R. Hassan, “Interference management in 5G and beyond network: Requirements, challenges and future directions,” *IEEE Access*, vol. 9, pp. 68932–68965, 2021.

[20] M. U. Khan, M. S. Sharawi, and R. Mittra, “Microstrip patch antenna miniaturisation techniques: A review,” *IET Microwaves, Antennas & Propagation*, vol. 9, no. 9, pp. 913–922, 2015.

[21] Ö. Yeniay, “Penalty function methods for constrained optimization with genetic algorithms,” *Mathematical and computational Applications*, vol. 10, no. 1, pp. 45–56, 2005.

[22] S. Mirjalili, S. M. Mirjalili, and X. S. Yang, “Binary bat algorithm,” *Neural Computing and Applications*, vol. 25, no. 3–4., pp. 663–681, 2013.

[23] S. Mirjalili and A. Lewis, “S-shaped versus V-shaped transfer functions for binary particle swarm optimization,” *Swarm and Evolutionary Computation*, vol. 9, pp. 1–14, 2013.

H. M. Kha received the B.E and M.E degrees in Electronics and Telecommunications Engineering both from Hanoi University of Science and Technology, in 2002 and 2004, respectively. He obtained his Dr.-Eng. (PhD) degree in Communications Engineering from the University of Paderborn, Germany in 2016. His research interests include digital signal processing, wireless communication, positioning engineering, machine learning, and pattern classification, and nature-inspired algorithm application.

T. V. Luyen received the B.S. and M.S. degree from the Hanoi University of Science and Technology, in 2002 and 2004, respectively, and the PhD degree from VNU University of Engineering and Technology in 2019. His research interests are in Beamforming and Beamsteering for antenna arrays, Smart Antennas, Optimum Array Processing, Nature-inspired Optimization Algorithms, and Artificial Intelligence.

N. V. Cuong received the B.E. and M.E. degrees both from Hanoi University of Industry, in 2020 and 2022, respectively. His research interests include beamforming for antenna arrays, smart antennas, nature-inspired optimization algorithms, convex optimization, and deep learning.